Multitask Molecular Springs: Collective Helical Vibrations of R_2S_n (R = H, C_6H_5, C_2H_3, CCl_3)—A Quantum Mechanical Study

George V. Papamokos[†] and Ioannis N. Demetropoulos*

University of Ioannina, Department of Chemistry, Sector of Physical Chemistry, Panepistemioupoli Dourouti, Ioannina, Greece

Received: July 11, 2001; In Final Form: December 3, 2001

The H_2S_n homologous series is proposed as a model for the collective vibrations of helical molecules. The polysulfane series was selected as the molecular set that resembles most closely a molecular discretization of a continuous helical curve. The computational vibration analysis for the levels of theory—MNDO, RHF/3-21G, RHF/6-31G*, RHF/6-31G**, MP2(FC)/6-31G*, and DFT B3LYP/6-31G*—revealed a number of collective vibrations. These vibrations resemble the motion of (a) a transverse wave, (b) a longitudinal wave, and (c) a transformation of the cylindrical shape to a breathing pulse, to an ellipsoidal-hyperboloidal, or to a cone. The precursor of a helical transverse wave is SSSS torsional vibrations, while SSS bending vibrations are the precursor of a longitudinal wave; finally, aggregated SS stretching is the precursor and generative force for the reported changes of the cylindrical helical shape (breathing, conical, ellipsoidal-hyperboloidal). The number of sulfur atoms and the hydrogen substitution were studied for their effects on appearance/disappearance of the characteristic helical vibrations. Also, they were studied for their effects on the overall molecular shape. The helical structure of polysulfanes is proposed to be ideally suited to provide a reference molecular prototype for classification of the low-frequency vibrations of helical biopolymers leading to global bend, global stretch, or breathing, conical, ellipsoidal-hyperboloidal transformations. Vibrations of this kind are particularly interesting for their biological and nanomechanical functions.

1. Introduction

Helical structure is very common in a great variety of molecules. The helical motif is found in many inorganic polymers.[1] The majority of the known crystal structures of organic polymers adopt a helical conformation.[2] In biopolymers, the existence of helical structure plays a key role in molecules of great significance such as DNA, proteins, and polypeptide chains.

Low-frequency vibrations of biopolymers are of great importance. It has been suggested that low-frequency vibrations produce motions that play a critical role in the biological activity of many biopolymers since they possess much more significant biological functions than the high-frequency motions.[3,4] Motions of this kind arise from a large part of the molecule even from all its atoms or, from the proper microenviroment.[5] Low-frequency vibrations may produce global bend, stretch or twist of the helix,[5] which are characteristic of the helical motif.

Both theoretical and experimental work have been carried out for the vibrational analysis of helical biopolymers and especially low-frequency vibrational analysis, including theories, algorithms and methods for the characterization, description, and formalism of such motions.[6−13]

The quantum mechanical calculation of the vibrational frequencies of biopolymers, though, requires large-scale computational resources due to the large number of the atoms that each monomer consists of. On the other hand, characterization, classification, and prediction of characteristic helical vibrations are important for the evaluation of the existing or proposed functionality of such motions not only in biopolymers but in a wide variety of chemical functions such as chemical kinetics, chemical reactions, or the new field of nanomechanics. A helical polymer being built from small units would be suitable though for this kind of analysis.

Polymeric sulfur forms helices.[14a,b] It has been used to test theories of the spatial configurations of chain molecules related to polymer statistics and critical phenomena.[15−17] Its structure and electronic properties have been studied theoretically in previous works.[18−20]

Sulfur, as a part of a polymeric chain, has the following advantages:

(i) It is very flexible since S−S bonds vary between 180 and 260 pm, depending partly on the character of the bond, S−S−S angles vary between 90° and 180°, while S−S−S−S adopt values between 0° and 180°.[14b]

(ii) The repeating monomer consists of only one atom that, additionally, does not aggravate the computations.

To achieve a reasonable number of sulfur atoms, the polysulfane series was chosen. It was also chosen for another reason: It represents a nearly ideal discrete spanning of a continuous regular helical curve. Of the wide variety of polysulfur compounds,[21] the polysulfanes are of great importance. R. Steudel and A. H. Otto, in their recent work on gas face acidities of H_2S_n (n = 1−4),[22] indicated that for a long time these species were only of academic interest until it was suspected that H_2S_2 is present in "sour gases"(see their ref 3) and higher members were detected in elemental sulfur produced from sour gas. In addition, many structural aspects can be studied in these compounds. Also, M. Schmidt and W. Siebert have pointed out that "...polysulfanes are the link of a very close

* Corresponding author. E-mail:idimitr@cc.uoi.gr. FAX: ++30-651-44989.

[†] E-mail: me00109@cc.uoi.gr.

10.1021/jp012653n CCC: $22.00
Published on Web 02/12/2002

genetic connection, elemental sulfur on one side, with all the many compounds containing sulfur−sulfur bonds in their molecules on the other side".[23] Most of our knowledge on these compounds stems from the elegant work of F. Fehér and his group in the 1950s. A continuously developing field of the chemistry of polysulfanes is that of organic polysulfanes R_2S_n.[21] A number of these substances adopt a helical conformation for the $C-S_n-C$ part.[21,24−26]

Experimental and theoretical data are available for the vibrational spectroscopy of H_2S_n[27−31] (helical or not), while for R_2S_n (helical or not), to our knowledge, there are only experimental data in the literature.[24,26,32,33] For the compounds above, the vibrational analysis is restricted to classic S−S, S−S−S and S−S−S−S vibrations. In one of the above works,[28] there is a calculation of phonon dispersion curves of the polysulfane series, which describes the optical and acoustical bands. Phonon dispersion curves give the variation of phonon energies with the phase difference between identical atomic displacements in neighboring chemical repeat units. They were calculated by Wilson GF method[34] as described by Higgs[35] for infinite helical polymers. A particularly useful adaptation of this method has been given by Peticolas et al.[29,36] Optical mode implies vibrations perpendicular to the chain, whereas the term acoustical mode implies a vibration in the direction of the chain. For mathematical rules and restrictions for the optical and acoustical branches, refer to the work of L. Piseri et al.[37]

In this work, H_2S_n is proposed as a model for the study of the vibrational motion of helical molecules using normal-mode analysis. Adopting polysulfanes as a model, the description and classification of characteristic helical vibrations become simple and can be summarized and applied to more complicated substances such as helical biopolymers in order to describe the motions that are expected to appear in a helical molecule. One could argue that when the H_2S_n series is used as a model many effects such as hydrogen bonding, atom or group interactions could not appear in such vibrations. The origins of these motions can also vary in different substances. The argument in favor of using H_2S_n series as a model is that many of these phenomena can be revealed either by the appearance of extra helical vibrations that are not expected or by the disappearance of an expected one in other substances.

As mentioned above, these motions are confirmed spectroscopically in many molecules. This work is exclusively focused on the existence and behavior of the helical vibrations. Their existence is confirmed in a series of molecules computed by applying various levels of theory.

Substitution of the terminal hydrogens with several organic molecules is also studied. One of them, $(CCl_3)_2S_7$ has been reported recently [synthesis, elucidation, X-ray characterization].[26] The results agree with those of H_2S_n series. Vibrational selection rules[38] where not applied for the normal modes since the aim was to collect all the kinds of vibrational motion and their subcategories in order to generalize the results for every helical molecule.

To our knowledge, it is the first time that longitudinal, transverse, breathing, conical, hyperboloidal-ellipsoidal vibrations are studied together on polysulfanes, while a systematic taxonomy has been developed. It is also the first time that helical polysulfanes are proposed as a model for the study of these vibrations.

Such motions will bring to mind continuum mechanics where a helix is treated as an elastic rod and helical springs of arbitrary shape whose natural frerquencies[39] are the subject of study.

2. Computational Methods

This section summarizes the combination of the H_2S_n and R_2S_n classes of molecules, the level of theory and the packages used for the geometry optimization and the calculation of the normal modes. The packages used are Gamess[40] installed at a small beowulf[41] cluster of pcs, PcGamess v(5.1)[42] of the gamess package[40] installed at an Intel PII 400 pc, and Gaussian98[43] installed at a 16 Origin2000 processors machine.

The calculations made use of the following theoretical descriptions: (a) semiempirical MNDO,[44] (b) abinitio RHF employing 3-21G,[45] 6-31G*,[46] and 6-31G**[46] basis sets of Gamess package, and (c) MP2(FC), where FC indicates a frozen core in the MP2 level while the B3LYP[47] functional was adopted for the DFT level of theory with 6-31G* basis set in the Gaussian98 package.

All molecules were subjected to a full-unconstrained optimization of their geometry under very tight optimization criteria. The initial starting point was an all 87.0 dihedral angle backbone of the S_n part of every molecule except $(CCl_3)_2S_7$, where the experimental geometry was adopted. The RSSS angle (R being carbon or hydrogen) was set at 90°; exceptional case was, again, the experimental value of $(CCl_3)_2S_7$.[26]

Frequencies were computed analytically except from the semiempirical level, where numerical procedures took place. The numbers of frequencies were scaled: RHF/3-21G results with the factor 0.9085, RHF/6-31*G results with the factor 0.8929, MP2(FC)/6-31*G results with the factor 0.9434, and B3LYP/6-31*G results with the factor 0.9613.[48]

Vibrations were visualized by Molden 3.6.[49] The vibrations of interest were chosen and their *X*, *Y*, *Z* atomic Cartesian translations gave the resultant translation for each atom separately. All the atomic resultants for each vibration were scaled linearly by a coefficient near to 50. The result was added to the optimized equilibrium *X*, *Y*, *Z* Cartesian coordinates of the molecule under study. By this method and with proper scaling, the picture of the molecule in its extreme position was achieved.

Altogether, 22 molecules have been treated.

(i) H_2S_n with $n = 4-12$, 21, 31, 41, 51. The H_2S_4 is the first molecule in the series that has a torsional angle fully consisted of sulfurs. The increment by one atom stops at $n = 12$. H_2S_{11} might show a repeat distance of 10 atoms according to the S∞ structure.[14] *N* values of 21, 31, 41, 51 were chosen since they follow an increment of 10 atoms at H_2S_{11} each time. Another reason that long polysulfanes have been treated is that in polysulfane series *n* can have values of 35 and above.[50] The H_2S_n series were treated with the following levels of theory (packages used are given in parentheses): H_2S_n of $n = 4-12$ was treated with MNDO (Pcgamess) and RHF/3-21G (Gamess). Additionally for $n = 4-8$: RHF/6-31G* (Gamess), RHF/6-31G** (Gamess), MP2(FC)/6-31G* (Gaussian98), and DFT B3LYP/6-31G* (Gaussian98) were applied. H_2S_{12} was also treated with DFT B3LYP/6-31G* (Gaussian98).

H_2S_n of $n = 11$, 21 were treated with MNDO (Pcgamess) and RHF/3-21G (Gamess). Also, for $n = 31$, 41, 51, the semiempirical level of MNDO (Pcgamess) was used.

(ii) R_2S_n, with R being C_2H_3 or C_6H_5 and $n = 5$, 7 (other organic polysulfanes are found with helical S_n parts, *n* being 5 or 7).[25,26] Molecules with $n = 11$, 22 are chosen in order to study the substitution effects in longer helical chains. Such a length for a sulfur chain should not be considered unusual since other compounds (chlorosulfanes) with up to 30 sulfur atoms have been detected by indirect HPLC analysis (after derivatization),[51] while organic polysulfanes with 9[52,53] and 11[32] sulfur atoms

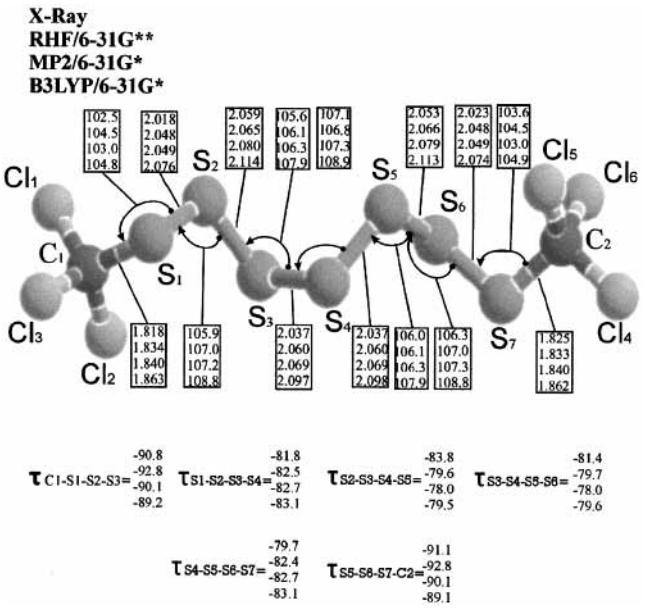

Figure 1. Numbering of atoms and structure of $(CCl_3)_2S_7$ from X-ray[26] and from present theoretical work.

have been synthesized (not necessarily in helical structure). The levels of theory and the packages used for the treatment of R_2S_n ($R = C_2H_3$ or C_6H_5) are given below:

For $n = 5, 7, 11, 22$, the MNDO (Pcgamess) was applied. Additionally, H_2S_5 and H_2S_7 were treated with RHF/3-21G (Gamess).

(iii) $(C\ Cl_3)_2S_7$ is a molecule, which has been synthesized and characterized by IR, Raman, and laser spectroscopy,[26] with a relatively long sulfur helical chain and terminal parts that do not aggravate the calculations. Experimental (X-ray) structural results produced by Steudel et al.[26] and theoretical structural results (RHF/6-31G*, MP2/6-31G*, DFT/B3LYP/6-31G*) produced in this work for the $C-S_7-C$ part of the molecule are given in Figure 1. Information about the deviation of the X-ray technique is given in Table 2 of ref 26. This molecule was treated with all levels of theory: MNDO (Pcgamess), RHF/3-21G (Gamess), RHF/6-31G* (Gaussian 98), RHF/6-31G** (Gaussian 98), MP2(FC)/6-31G*, and DFT B3LYP/6-31G*.

Several studies[54−60] have shown that vibrational frequencies calculated using DFT methods agree well with experiment and are much superior to the Hartree−Fock (HF) theory. Studies on molecules containing sulfur[61,62] including H_2S and H_2S_2 molecules,[62] which compare results with MP2 treatments, recommend the use of DFT methods, particularly the hybrid methods such as B3LYP, for reliable prediction of frequencies when no hydrogen bonding is present.

In this case, from the structural point of view, the RHF/3-21G geometry optimization of H_2S_7 and $(CCl_3)_2S_7$ molecules (Table 1S) yields results surprisingly close to the DFT/B3LYP/6-31G* dihedral angles, maybe due to errors' cancellation, while MNDO is useful mainly as a trend indicator. So RHF/3-21G seems to be a quite accurate approximation of the dihedral angles in helical sulfur. This is confirmed from calculations on H_2S_n series, n being 4−8, 12 (results available upon request from the authors).

3. Results and Discussion

The section is organized in two parts. In part A the helical shape modifications due to (a) terminal group R and (b) to the length of the sulfur chain are discussed. The main body of the work is in Part B where the polysulfane series is presented and analyzed as molecular vibrating springs.

A. Structural Aspects of the Helical Molecular Form of the R_2S_n Molecules. Before any proceeding, it should be clarified that H_2S_n and R_2S_n molecules are studied as helical. This is one of the many expected conformational isomers of a polysulfane and some of them are of the same total energies.[27,63,64] Polysulfanes, in their crystals, adopt only one of these conformers, but in their melts, they adopt several. Thermodynamically, according to R. Steudel et al.,[33] who accounted for low melting points of specific organic heptasulfanes, this leads to long chain polysulfanes being either liquid or having melting points only slightly above ambient temperature. $(C\ Cl_3)_2S_7$ is a molecule which adopts a helical conformation in its crystal.

The cylindrical surface that circumscribes the molecular helix is affected by replacing hydrogen with various substitutes. Here, the structures of H_2S_7 with R_2S_7 ($R = C_2H_3$, C_6H_5, CCl_3) were used as models for comparison (all structural data are given in Table 1S).

1. Structural Effects from Substitution. It is observed that the main structural difference stems from dihedral angles, which are related to the substituent ($X_1-S_1-S_2-S_3$, $S_1-S_2-S_3-S_4$, $S_4-S_5-S_6-S_7$, $S_5-S_6-S_7-X_2$). Contrarily, the dihedral angles of long chain molecules, which are not close to the substituent, hold their values close or identical to those of H_2S_n series.

In general, substitution may cause a raise, or a reduction of the value of the particular dihedral angles. It may also be neutral. This causes some changes to the radius of the helix. The radius can (a) increase, (b) decrease, (c) stay unchanged, or (d) increase and decrease simultaneously in adjacent or nonadjacent parts of the helix.

Changes in the curvature or the pitch of a helix can also be observed. All these changes can result in different structural categories of helices. Biohelices are one example, which are characterized as α-helices, 3_{10} helices, etc. These changes can also result in the loss of the helical character if the circumstances permit it.

Apparently, the shape of the helix is a matter of chemistry. Any shape of a helix can be achieved if the proper substitution takes place. Electron withdrawing, nucleophilicity, p-system presence, electronegativy, and many other electronic or steric reasons familiar to every chemist can cause this change. So a regular helix transforms to ellipsoidal or hyperboloidal helical curve and vice versa. It also may transform to conical if different substances substitute the two ending hydrogens. Many other shapes can appear depending on the substituents. Being able to construct helices with predefined shape is a challenge for a theoretical or experimental chemist.

In this work, the motives of the helix being regular (cylindrical), ellipsoidal (barrel like), hyperboloidal, and conical are determined and are demonstrated:

Comparison of H_2S_7, R_2S_7. The optimized structures of H_2S_7 and R_2S_7, with R being C_6H_5, C_2H_3, and CCl_3, are given as a pictorial representation in Figure 2 (R = H, MP2/6-31G*; R = C_6H_5, RHF/3-21G; R = C_2H_3, RHF/3-21G; R = CCl_3, MP2/6-31G*). See also Table 1S of the Supporting Information. HF/3-21G shows a reduction of $X_1-S_1-S_2-S_3$ and a reduction of $S_1-S_2-S_3-S_4$ value when C_2H_3 substitutes hydrogen. The same is observed for the symmetrical dihedral angles on the other side of the molecule. The helix is almost regular (Figure 2IIA).

HF/3-21G results for H_2S_7, Phe_2S_7 show an $X_1-S_1-S_2-S_3$ and an $S_1-S_2-S_3-S_4$ reduction when H is substituted by C_6H_5.

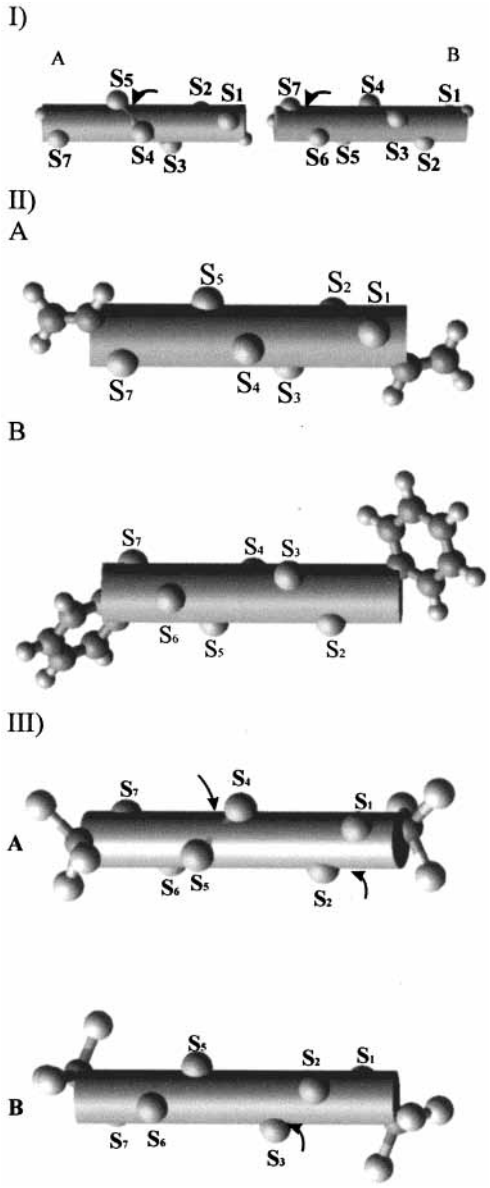

Figure 2. (I) H_2S_7 minimized at MP2 /6-31G* level of theory. Snapshots of the molecule as it turns around its axis. Note how atoms and bonds in the middle are exerted while in the two ends all bonds are under the cylinder and the atoms are inner. (II) R_2S_n (R = Ethylene, C_6H_5, $n = 7$) at the HF/3-21G level of theory. The helix transforms to a regular one by this substitution. The S_3 and S_5 atoms are slightly exserted with C_2H_3. The difference is impalpable and the helix is almost regular. For C_6H_5, a perfect regular helix of the Sn part is formed. (III) $(CCl_3)_2S_7$ minimized at MP2 /6-31G* level of theory. Snapshots of the molecule as it turns around its axis. Note again how atoms and bonds in the middle are exerted, while in the two ends they are not, following the H_2S_7 trend.

The two terminal dihedral angles ($X_1-S_1-S_2-S_3$, $S_5-S_6-S_7-X_2$) are smaller than the others in the middle, which remain almost the same despite the substitution. The helical Sn part becomes a regular helix (Figure 2IIB).

$(CCl_3)_2S_7$, a left-handed molecule, shows an increase of $X_1-S_1-S_2-S_3$ and an $S_1-S_2-S_3-S_4$ value in all levels with the exception of MNDO, which systematically fails. The S_n helical part continues to have ellipsoidal characteristics (Figure 2IIIA,B)

The R_2S_7 molecule has six dihedral angles. Let $X_1-S_1-S_2-S_3$ be a_1 dihedral angle, and let $S_5-S_6-S_7-X_2$ be a_6 dihedral angle. Then $S_i-S_{i+1}-S_{i+2}-S_{i+3}$ ($i = 2-5$) corresponds to a_i.

The above definition of sequence of dihedral angles should fulfill certain constraints in order to create a particular helical shape:

(i) The pattern for a perfect regular helix should satisfy the relation $a_1 = a_3 = ... = a_6$.

(ii) The pattern for a conical helix should satisfy the inequality constraints $a_1 < a_2 < a_3 < a_4 < a_5 < a_6$.

(iii) The pattern for an ellipsoidal (barrel like) helix should satisfy the relations $a_1 > a_2 > a_3 = a_4 < a_5 < a_6$.

(iv) The pattern for a hyperboloidal helix should satisfy the relations $a_1 < a_2 < a_3 = a_4 > a_5 > a_6$.

Figure 2 depicts the regular and hyperboloidal patterns of H_2S_7 and R_2S_7 molecules.

2. Structural Effects by Raising the Number of S Atoms. To study the effects of increasing the S atoms of the helix in H_2S_n series, the computed geometrical results for $n = 4-8$ are summarized as it follows:

Studying the H_2S_n series for $n = 4-8$, one can conclude that no significant structural changes are observed. Increments of the chain length influence the geometrical characteristics very little. The results agree with the work of ref 28. The H−S bond remains the same with an MP2 value of 1.3448−1.3450 Å. The H−S−S angle is 98.7° everywhere. The H−S−S−S angle has a MP2 value of 84.2−84.7°. The S−S bond has a value equal or very close to 2.07 Å, slightly smaller than the accepted 2.08 Å length. S−S−S angles vary between 107.5° and 107.0° and S−S−S−S angles between 84.7° (terminal) and 78.1° (in the middle), keeping the trend to increase in ending parts. This is an interesting point. Raising *n* causes the cylinder to adopt a particular shape related to the trend of the torsional angles. This shape becomes clear with molecules having two or three turns such as H_2S_7 and is expected to be maintained at even longer since the end effect is very weak to influence the angles in the middle.

B. Vibrational Analysis. *1. Literature Survey.* After an extensive search of the literature, experimental and calculated frequencies for H_2S_n and R_2S_n became available and are discussed.

The calculated SSSS torsional frequencies in the RHF/6-31*,[29] RHF/6-31**,[28,29] MP2(FC)/6-311G**,[27] and PP/PSEUDO[28] levels of theory mainly for $n = 4-6$ of the H_2S_n series, lie in the region 35−75 cm^{-1}. The experimental SSSS torsional frequency of H_2S_4 lies at 77 cm^{-1} of the spectrum.[31b]

The SSS bending frequencies lie in the region 149−242 cm^{-1} of the Raman spectrum[30,31a] and in 131−283 cm^{-1} of theoretical treatment.[27−29] Finally, SS stretching frequencies are found in the 439−485 cm^{-1} region of Raman spectrum[30,31a] and in the 432−560 cm^{-1} region of theoretical treatment. [27−29]

Where unscaled, the calculated values were compared with the experimental values based on the relative ordering of frequencies than on absolute values.

The frequency values of organic polysulfanes[26,32,33] concern SS stretching and SSS bending vibrations. In general, the values are the same or very close to the regions of the H_2S_n series. For $(CCl_3)_2S_7$,[26] its six SS stretching modes result in three Raman signals. The writers[26] ascribe this fact to incidental degeneracies and to the presence of the very strong symmetrical $SCCl_3$ stretching vibration (436 cm^{-1}). The same phenomenon occurs to the sulfur compound of ref 32. The number of SS stretching modes are smaller than the expected, a fact which is ascribed to coincidental degeneracies. These frequencies can be used to account for the number of S atoms of a sulfur chain. (For a full tabulated report on the findings of the literature, see Tables 2S, 3S, 4S.)

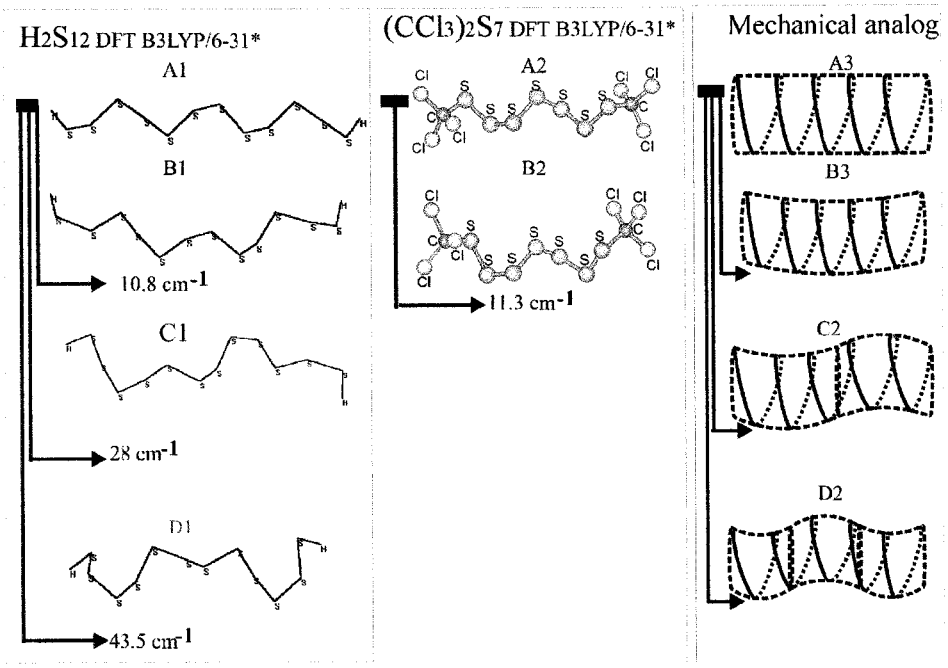

Figure 3. Helical bend 1c, helical bend 2c, and helical bend 3c. For $(CCl_3)_2S_7$, the helical bend 2c exists at 31.4 cm^{-1}, while the helical bend 3c does not exist.

2. Present Work. This work aims to describe vibrations that were observed to produce motions that resemble a longitudinal wave, a transverse wave, or a helical shape transformation. Each characteristic vibration will contain:

(i) Report, general discussion of the vibration.

(ii) Molecular representation using the H_2S_{12} and the $(CCl_3)_2S_7$ molecules in their extreme positions as they oscillate during the vibration at the DFT level of theory. The H_2S_{12} molecule was chosen because every kind of collective motion described below is clear and existent on it, while on smaller molecules of the H_2S_n series such as H_2S_4 or H_2S_5, only the generic factor can be seen. The $(CCl_3)_2S_7$ molecule was selected because it is a long organic polysulfane, which is solid and adopts a helical conformation as supported by X-ray examination.[26] $(CCl_3)_2S_7$ will be present as a figure in the first vibration of each category. Schematic representation of the molecule as a mechanical spring will also be available. (A drawing of an ideal spring showing the equilibrium position and its transformation when the oscillation reaches the extreme position.)

(iii) Calculated frequencies at which the collective motion is observed. Only DFT B3LYP/6-31* frequencies are given since all other methods for all molecules have resulted in the same collective motion that DFT describes; plus, identical conclusions stem from all elaborated computations. All other calculated frequencies for all methods and molecules are given as Supporting Information.

The vibrations are allocated in three categories:

(i) Helical bend: the helix is bending, and molecular curves are formed. If the symbol 1c follows, then an arc is formed. If the symbol is 2c, then two curves are formed, and a sin bend is produced, limited between $[0,2\pi]$. For every c added, the bound increases by one π. The motion resembles a standing transverse wave.

(ii) Helical stretch: The helix is stretching and regions of rarefaction are formed. If the 1r symbol follows, then 1 region of rarefaction is formed. If the symbol is 2r, two regions of rarefaction are formed. The motion resembles a longitudinal wave and the rarefaction gives rise to the definition of the wavelength of this standing wave.

(iii) Helical cylindrical shape transformation: The helix expands its radius uniformly, resembling a breathing pulse. If an asymmetric expansion takes place, then an ellipsoidal-hyperboloidal or a cone is formed.

3. Helical Bend 1c. Figure 3B shows the bending characteristics of vibration in the 3 prescribed ways. All molecules and methods substantiate this kind of motion. Studying Figure 3B, one can conclude that the helix is bending and one main helical curve is formed when the vibration reaches its extreme position. The molecular axis resembles an oscillating string, a standing transverse wave. It is always the first normal mode that generates this motion. DFT frequencies are as follows:

For $n = 4$, the frequency is 69.5 cm^{-1}; H_2S_5 has the characteristic excitation at 41.5 cm^{-1}, H_2S_6 at 30.8/41.9 cm^{-1}, H_2S_7 at 26.6/30.1 cm^{-1}, H_2S_8 at 24.1(degenerate)/25.0 cm^{-1}, H_2S_{12} at 10.8(degenerate)/12.6 cm^{-1}, and $(CCl_3)_2S_7$ at 11.3/13.2 cm^{-1}.

The precursor of this motion is the S−S−S−S torsional vibration in H_2S_4(69.5 cm^{-1}). The second normal mode of H_2S_6 (its next S−S−S−S torsional mode: 41.9 cm^{-1}) generates a similar motion. The precursor of this similar motion is the S−S−S−S torsional vibration, the second normal mode of H_2S_6. The difference between these two modes (examined as a global effect on the molecule) is the direction of the oscillation. Direction of normal mode 1 is almost vertical to the direction of normal mode 2. H_2S_5 does have a second normal mode, which is torsional, but its length does not permit the helix to oscillate in the described way uniformly. The difference in frequencies between these two modes gets smaller from H_2S_6 to H_2S_{12}, and in longer molecules of the H_2S_n series ($n = 8, 12$), these two modes are degenerate.

In even longer molecules, such as H_2S_{31} and R_2S_{22} ($R = C_2H_3$, C_6H_5), the second normal mode ceases to generate this kind of motion. This is supported by semiempirical and HF results. After $n = 8$, the mode that produces the motion is always degenerate for every method.

The main effect on the helix is the bending of its axis. Across the H_2S_{12} helical axis, the S_1 and S_{12} atoms oscillate almost antiparallel to the S_7 and S_8 atoms. Also, the ending sulfur atoms

represent the two edges of the wave while the sulfurs in the middle represent the top of it. Given the fact that the translations of the former are of 0.08 Å and the latter of 0.06 Å, the height of the wave of the vibration is estimated close and less than 0.14 Å.

It is also observed that frequencies move to lower values as the chain length increases. This comes in agreement with biomolecular behavior since helical bending is observed both in DNA[8] and polypeptide chains.[11] The same principle is followed in classical mechanics. Finally, the calculated frequency of H_2S_4, at the DFT level of theory, deviates 8 cm^{-1} from the experimental value.

4. Helical Bend 2c. The behavior of H_2S_{12}, as it vibrates at the DFT level of theory and the mechanical analogue of the helical spring are shown in Figure 3C1,2. In Figure 3C, the helix is bending, and two main curves are formed. The molecular axis resembles a transverse wave, a sin curve $(0,2\pi)$. This kind of motion first appears at the H_2S_7 molecule as a torsional SSSS vibration, and it is the precursor for longer sulfanes. It becomes clearer at higher members of the series.

DFT frequencies are as follows:
For $n = 7$, the frequency is 44.3 cm^{-1}; for $n = 8$, we meet the characteristic excitation at 52.8 cm^{-1}. H_2S_{12} exhibits the motion in two frequencies: 28.0 and 30.2 cm^{-1} and $(CCl_3)_2S_7$ at 31.4 cm^{-1}.

H_2S_9 (treated with MNDO and RHF/3-21G levels of theory as mentioned in computational methods section) shows another similar vibration. It is vertical to the direction of the first one. This identical phenomenon was met at the first vibration that was described above but now it does not disappear in longer molecules such as H_2S_{21} and continues up to H_2S_{51}. MNDO gives rise to three modes with similar motion at R_2S_{11} ($R = C_6H_5$). The precursor for this vibration is the SSSS torsional vibration of H_2S_9. This accounts for the two numbers given above for H_2S_{12}.

The behavior of frequency depending on the number of sulfurs is to decrease as *n* rises. This behavior is obvious for someone who examines the results of MNDO and RHF/3-21G. (Table 6S). The highest frequency is observed at H_2S_8. Proceeding to longer molecules, the frequency falls progressively. The exception of this observation comes from H_2S_7. This molecule has a lower value of frequency than that of H_2S_8 in every level of theory. This does not mean that number seven or eight are critical points of the H_2S_n series. Probably the origin of the vibration of H_2S_7 stems from higher SSSS torsional frequencies than those of H_2S_8. Finally, the degeneracy is present everywhere in the longer molecules($n > 10$).

5. Helical Bend 3c. Figure 3D1 reproduces the motion of H_2S_{12} at the DFT level while Figure 3D2 gives the mechanical analogue. The helix is bending, and three main curves are formed. The molecular axis resembles again an oscillating string. This time the standing transverse wave resembles a sin curve increased by one π $(0,3\pi)$ compared to the previous bend.

This motion starts to appear at H_2S_{11} and it becomes clear at longer polysulfanes. Due to this fact, only the number of H_2S_{12} is presented at DFT level, which is 43.5 and 67.0 cm^{-1}. The direction of motion of the former is vertical to the direction of the latter.

The precursor of this vibration is the S−S−S−S torsion of H_2S_{11}. From H_2S_{12}, another similar motion appears and continues to higher members. It is, as mentioned before, vertical to the direction of the first one. The phenomenon is clear at the H_2S_n series with $n = 21, 31, 41, 51$. The degeneracy is intense in this vibration. This is a motion that is shown in higher members of helical polysulfane series. R_2S_{11} ($R = C_6H_5$) shows two modes that induce similar conformational change. The origins of these two frequencies are separate SSSS torsional vibrations.

Frequencies move lower as *n* increases. This is a general trend in helical bending. It is also observed in motions with more curves (4c, 5c, etc.) that appear in very long polysulfanes ($n = 21, 31, 41, 51$).

6. Helical Stretch 1r. Figure 4B picturizes the helical stretch 1r with H_2S_{12} and $(CCl_3)_2S_7$. The mechanical analogue is also given. The helix is stretching and the oscillation has the characteristics of a longitudinal wave. The center of the molecule shows rarefaction, which transforms to condensing. The motion is absolutely symmetrical.

The characteristic DFT frequency for H_2S_4 is 162.6 cm^{-1}. H_2S_5 vibrates at 123.6 cm^{-1}, H_2S_6 at 105.2 cm^{-1}, H_2S_7 at 89.6 cm^{-1}, H_2S_8 at 87.8 and 75.4 cm^{-1}, H_2S_{12} at 53.1 cm^{-1}, and $(CCl_3)_2S_7$ at 175.7 and 199.4 cm^{-1}.

The precursor of this motion is SSS bending in the H_2S_4 molecule (162.6 cm^{-1}). In longer molecules, the motion becomes clear. Degeneracies become dominant. Substitution affects slightly the appearance of the motion. In $(CCl_3)_2S_7$, it appears in higher frequencies than expected, while in R_2S_n for $n = 22$, it disappears, as observed at MNDO level. There is a bending character of this motion, but it is very small, and it should not be confused with the bending of the axis observed in the vibrations above. It is probably inevitable to have escort motions when these vibrations occur. They stem from the structural changes that vibrations produce. In biomolecules though mixed character is common. In DNA,[8] the first helical bending is also the first helical stretching. Helical stretch is observed in polyalanine and deoxymyoglobin.[10]

Frequencies become lower again as *n* increases, and it seems to be possible to predict frequencies at which helical stretch or bend can appear, with proper fitting.

7. Helical Stretch 2r. In Figure 4C, the helix is stretching resembling again a longitudinal wave. The left and the right part of the molecule now show one rarefaction each, which transforms to condensing. The transformation of the two regions is asymmetric as it is shown in the Figure 4C. The whole molecular motion is obviously asymmetric.

The characteristic DFT frequencies for H_2S_4, H_2S_5, H_2S_6, H_2S_7, H_2S_8, H_2S_{12}, and $(CCl_3)_2S_7$ are 202.7, 229.4, 187.6, 166.4, 145.7, 100.8, and 112.3/151.7 cm^{-1}, respectively.

This motion appears first in the H_2S_4 molecule as a precursor by an SSS bend. In the longer molecules, the motion becomes clear although the degeneracies appear. $(CCl_3)_2S_7$ vibrates this way in two frequencies. Except $(CCl_3)_2S_7$, which shows this motion at two frequencies, there is no other indication for a second normal mode, which generates such a vibration. This observation applies to the previous helical stretch (1r) as well. The phenomenon of two normal modes generating the same helical transformation, as it was met at helical bend, is not met in helical stretch.

Numbers are falling as *n* increases. In long molecules such as H_2S_{12} or longer, slightly mixed character of the vibration is observed when they are visualized. The characterization of motion though is very easy and clear as a helical stretch 2r.

8. Helical Stretch 3r. Figure 4D describes the motion as a longitudinal wave is formed again having three regions of rarefaction. The left and the right part of the molecule show one rarefaction each, which transforms to condensing, while the middle part of the molecule shows one condensing that transforms to spacing. The transformation of the two terminal

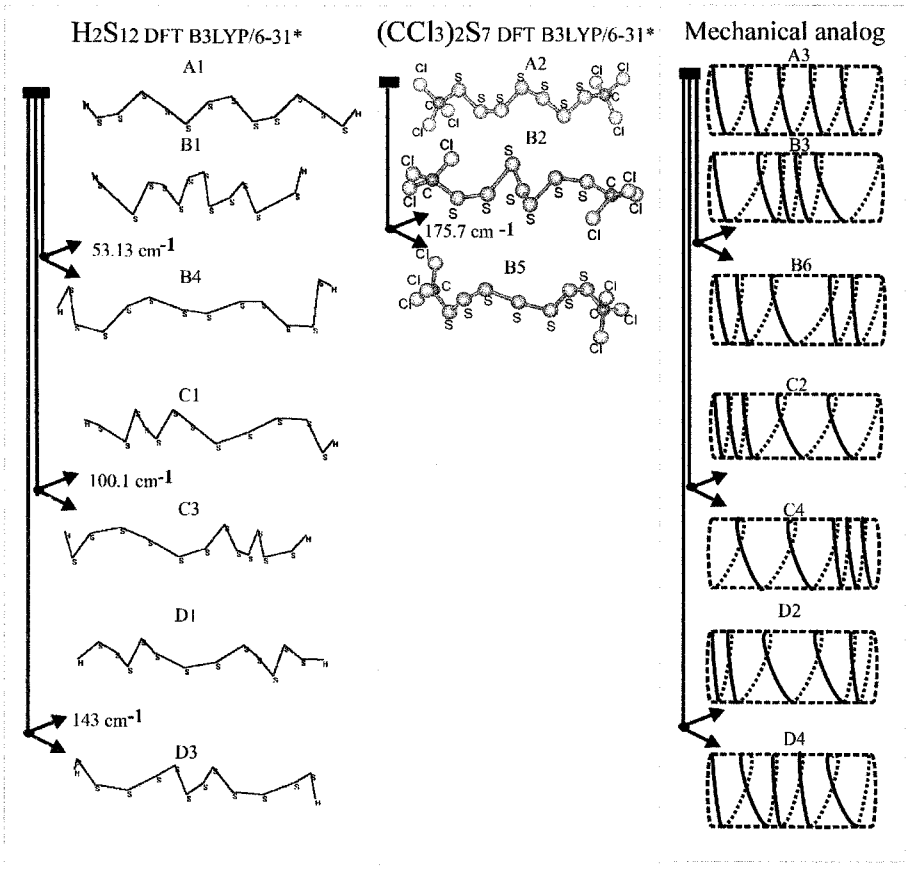

Figure 4. Helical stretch 1r, helical stretch 2r, and helical stretch 3r. For $(CCl_3)_2S_7$, the helical stretch 2r exists in 113.9 and 151.5 cm^{-1}, while the helical stretch 3r does not exist.

regions is asymmetric to the middle part, as the figure shows. The whole molecular motion is symmetric. Rarefaction appears one per three atoms. Regions of rarefaction are increasing along the helical chain. So we can meet motions with 3, 4, 5, etc., regions of rarefaction as the chain gets longer.

Results in the DFT level are available for H_2S_8 and H_2S_{12}. There is a degenerate mode at 205.7 cm^{-1} for the former and a mode at 143.0 cm^{-1} for the latter.

This motion appears first in the H_2S_8 molecule as a precursor. In smaller molecules a symmetric S−S−S bend exists, but it has local characteristics and does not generate the motion, as it should be. Inevitably, the SSS bend mode of H_2S_8 is the first in the series that produces the helical stretch 3r.

Frequencies are getting smaller as n increases and give rise for speculations about mixed character since the values drop in the region of SSSS torsional modes. Nevertheless, the whole molecular motion is a clear helical stretch.

9. Helical Breathing. The radius r of the helix oscillates between r_1 and r_2, where $r_1 < r_{equil} < r_2$ and the oscillation has the characteristics of a breathing oscillation of a cylinder. Figure 5B explains this motion at DFT level of theory. Note how the radius of the cylinder becomes slightly smaller in H_2S_{12} and $(CCl_3)_2S_7$. In most molecules, the two last S atoms are not parts of this motion. All the other S atoms are part of this motion that is symmetric.

H_2S_4, H_2S_5, H_2S_6, H_2S_7, H_2S_8, H_2S_{12}, and $(CCl_3)_2S_7$ vibrate at 445.4, 447.3, 423.3, 423.5 (degenerate), 423.5 (degenerate), 421.1, and 427.6 cm^{-1} of DFT level of theory, respectively. Full report of all numbers is given in Table 11S.

The generator of this transformation is S−S stretch. The precursor of this motion is H_2S_4. This motion is observed at every molecule, and it does not depend on the number of sulfur atoms. Surprisingly, $(CCl_3)_2S_7$ does not show this motion in MP2 6-31* level of theory although S−S stretching modes are present. The vibration is generated by one mode in any case.

Now the frequency of the motion does not drop when n increases but it just changes a band. It shifts to 423 cm^{-1} from 445 cm^{-1}. It is clear that the helical breathing is expected in the frequency region of SS stretch.

10. Helical Cone. The radius of the helix increases at the one end and decreases at the other forming a cone (Figure 5C). The whole molecular motion is asymmetric, but the shape of cone is generated uniformly.

The frequencies for H_2S_4, H_2S_5, H_2S_6, H_2S_7, H_2S_8, H_2S_{12}, and $(CCl_3)_2S_7$ are 450.7, 449.6, 446.7, 423.4/ 447.5, 424.6-(degenerate)/448.5(degenerate), 423.2(degenerate), and 456.0 cm^{-1} of DFT level of theory, respectively.

This transformation is generated from asymmetric S−S stretch since all the frequencies are in the S−S stretch region. For n = 3−6 of the H_2S_n series, the S−S stretch of the last S−S bond of each part of the helix, aided by escort S−S stretch in the middle of the helix, generates this motion. For $n = 7$, 8, another S−S asymmetric stretch generates a second similar transformation which is observed only in the highest levels of theory DFT, MP2. The latter replaces the former in even longer molecules. Substitution affects the appearance of two similar transformations as is it shown by the comparison of H_2S_7 and $(CCl_3)_2S_7$ in DFT level.

The numbers now lie again in two bands: the first is near 450 cm^{-1} and the second is close to 425 cm^{1}. Both regions are active for SS stretching as supported by the literature survey.

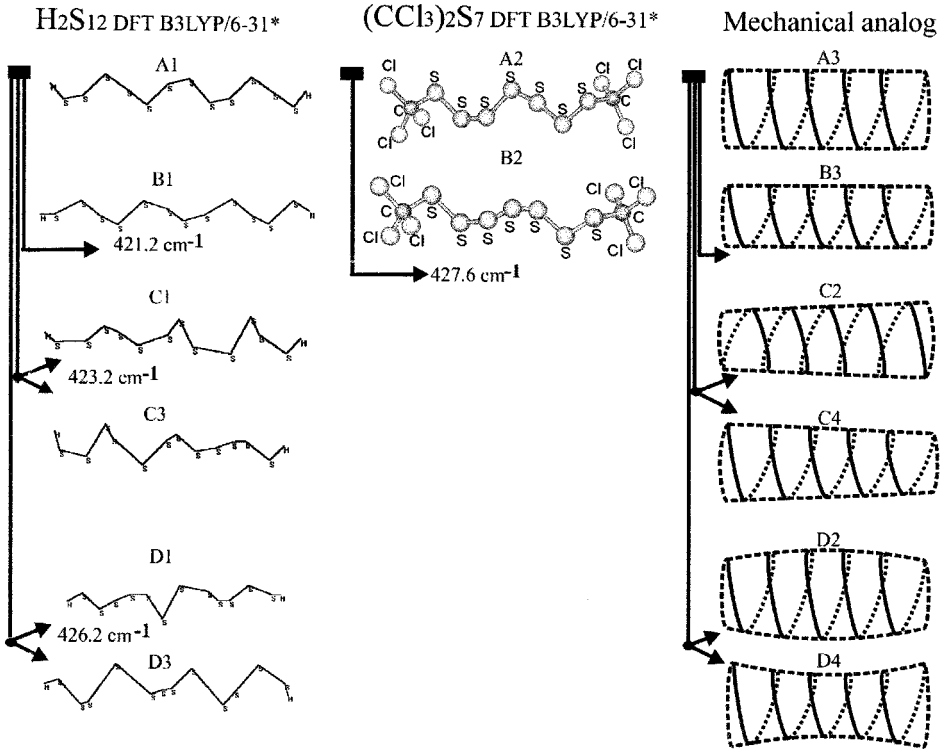

Figure 5. Cylindrical transformations: Breathing, conical, and hyperboloidal-ellipsoidal vibrations. For $(CCl_3)_2S_7$, the conical vibration exists at 456 cm^{-1}, while the hyperboloidal-hellipsoidal does not exist.

11. Helical Hyerboloidal-Ellipsoidal. The behavior of the helix now is to increase its radius at the two ends and, simultaneously, to decrease it at the middle and vice versa (Figure 5D). The helix transforms to a hyperboloidal that shifts to an ellipsoidal when the two extreme positions of the oscillation alternate. The molecular vibration is symmetric.

This is a transformation that only higher members of the series show. In general, this means that a particular number of sulfurs are needed in order the vibration to show up.

H_2S_8 shows this motion in RHF and MNDO but not in MP2 and DFT levels of theory. Thus, only the number of H_2S_{12} at the DFT level is presented, which is 426.0 cm^{-1}.

This transformation is also generated by the S−S stretch. In this case, the precursor cannot be clearly reported since MP2 and DFT do not support H_2S_8 that other levels do. On the basis of previous results, the precursor should be between H_2S_8 and H_2S_{10}.

In general, the S−S stretch calculated bands are in agreement with the experimental regions of H_2S_n and R_2S_n.

Conclusions

The main findings of this work are summarized as follows.

The polysulfane family of compounds is proposed here to serve as a prototype for studying the global transformation of the helical cylindrical shape, the global bend or stretch of a molecular helix since it represents a discrete spanning of a continuous helical curve without the distractions of side attached atoms.

The computational study of the helical polysulfanes using a wide range of levels of theory [MNDO, HF/6-31G, HF/6-31G*,-MP2/ 6-31G*, DFT-B3LYP/ 6-31G*] in applying normal mode vibrational analysis discover global helical bend attributed to collective S−S−S−S torsions. Helical bend *k*c [$k = 1-3$] has been observed where the long molecular axis globally assumes a transverse wave of the form of a sin curve $(0,k\pi)$ [$k = 1-3$]. Global helical stretch kr has been recognized as an aggregate of coordinated S−S−S local bending vibrations building to a longitudinal wave also for $k = 1-3$. The orchestrated individual S−S stretches have been identified to produce (i) global helical breathing where the radii of the turns uniformly oscillate, (ii) transformation of a cylindrical to conical helix, and (iii) transformation of a cylindrical helix to hyperboloidal helix. This systematic documentation of the helical molecular vibrations came up for the first time, to our knowledge, with helical vibrations yielding conical, hyperboloidal, and ellipsoidal helices.

As *n* rises, more helical bending, stretching, and cylindrical transformations will appear. So in higher members of the series such as H_2S_{35}, a helical bend of 3c, 4c, 5c, and so on is expected as well as for helical stretching (3r, 4r, 5r). These expectations are based on MNDO computations for H_2S_n [$n = 21, 31, 41, 51$]. Longer molecular helices certainly could provide more waves spanning the molecule (higher values for *k*).

The frequencies of longitudinal and transverse transformations exhibit a decrease as the number of sulfur atoms increases.

The frequencies of breathing, conical, and hyperboloidal vibrations show to be nearly invariant as the number of sulfur atoms *n* increase to a value; then the frequencies sustain an abrupt decrease by ~20 cm^{-1} and remain constant against further *n* increases.

Substances such as helical polymeric selenium, polysilane, and polyethylene are proposed for the study of the vibrations described in this work. The geometry of these substances are governed by similar factors.[18,19,65]

The interest in low-frequency vibrations has been stimulated by the discovery of a 15 cm^{-1} vibration coupled to a functional electronic transition in a photosynthetic reaction center.[66] New experimental techniques are developed for the detection of low-frequency vibrations. This systematic analysis of the coordinate movements of the individual atoms belonging to a helical shaped

molecule, which can be recognized as a "molecular" wave, transverse or longitudinal, can also reveal another potential function. Such a molecular spring, in a proper surface potential, can be an example of atomic scale engines described recently.[67,68]

Supporting Information Available: Tables of dihedral angles and frequencies.. The material is available free of charge via the Internet at http://pubs.acs.org.

References and Notes

(1) Wells A. F. *Structural Inorganic Chemistry*; Clarendon: Oxford, 1984.

(2) Tadokoro, H. *Structure of Crystalline Polymers*; Wiley: New York, 1979.

(3) Peticolas, W. L.; Dowley, M. W. *Nature* **1966**, *212*, 400.

(4) McCammon, J. A.; Gelin, B. R.; Karplus, M.; Wolynes, P. G. *Nature* **1976**, *262*, 325.

(5) Chou, K. C. *Biophys. J.* **1984**, *45***,** 881.

(6) Lee, S. H.; Krimm S. *Chem. Phys.* **1998**, *230*, 277.

(7) Lee, S. H.; Krimm S. *Biopolymers* **1998**, *46*, 283.

(8) Duong, T. H.; Zakrzewska K. *J. Comput. Chem.* **1997**, *18*, 796.

(9) Donghai, L.; Matsumoto, A.; Nobuhiro G. *J. Chem. Phys.* **1997**, *107*, 3684.

(10) Corbin, S. F.; Smith, J. C.; Lavery, R. *Biopolymers* **1995**, *35*, 555.

(11) Peticolas, W. L. *Biopolymers* **1979**, *18*, 747.

(12) Fanconi, B.; Small, E. W.; Peticolas, W. L. *Biopolymers* **1971**, *10***,** 1277.

(13) Itoh, K.; Shimanouchi, T. *Biopolymers* **1970**, *9*, 383.

(14) (a) For a survey in sulfur, see: Donohue, J. *The Structures of the Elements*; Wiley: New York, 1974; Chapter 16. (b) Greenwood, N. N.; Earnshow, A. *Chemistry of the Elements*, 2nd ed.; BH: London, 1997; Chapter 15.

(15) Mark, J. E.; Curro, J. G. *J. Chem. Phys*. **1984**, *80*, 5262.

(16) Tuinstra, F. *Acta Crystallogr*. **1966**, *20*, 341.

(17) Lind, M. Geller, S. *J. Chem. Phys*. **1969**, *51*, 348.

(18) Cui, C. X.; Kertesz, M. *J. Am. Chem. Soc*. **1989**, *111*, 4216.

(19) Springborg, M.; Jones, R. O. *J. Chem. Phys.* **1988**, *88*, 2652.

(20) Springborg M.; Jones, R. O. *Phys. Rev. Lett.* **1986**, *57*, 1145.

(21) Steudel, R.; Kustos, M. *Encyclopedia of Inorganic Chemistry*; Wiley: Chichester, 1994; Vol. 7.

(22) Otto, A. H.; Steudel, R. *Eur. J. Inorg. Chem.* **1999**, 2057 and references therein.

(23) Schmidt, M.; Siebert W. *Comprehensive Inorganic Chemistry*; Pergamon Press: Oxford, 1973; Vol. 2, Chapter 23, p 826.

(24) Minkwitz, R.; Kornath, A.; Preut, H. *Z. Anorg. Allg. Chem*. **1994**, 981 (especially Tables 5 and 6).

(25) Kustos, M.; Pickardt, J.; Albertsen, J.; Steudel, R. *Z. Naturforsch. B* **1993**, *48*, 928.

(26) Steudel, R.; Pridöhl, M.; Buschmann, J.; Luger P. *Chem. Ber*. **1995**, *128*, 725.

(27) Drozdova, Y.; Miaskiewicz, K.; Steudel, R. *Z. Naturforsch*. **1995**, *50b*, 889.

(28) Birner, P.; Köhler, H. J.; Karpfen, A.; Lischka, H. *J. Mol. Structure* **1991**, *91*, 223.

(29) Cui, C. X.; Kertesz, M. *J. Chem. Phys.* **1990**, *93*, 5257 (especially tables II and VI).

(30) Fehér, F.; Laue, W.; Winkhaus, G. *Z. Anorg. Allg. Chem.* **1956**, *288*, 103.

(31) (a) Fehér, F.; Laue, W. *Z. Anorg. Allg. Chem.* **1956**, *288*, 113. (b) Wieser, H.; Krueger, P. J.; Muller, E.; Hyne, J. B. *Can. J. Chem*. **1969**, *47*, 1633.

(32) Steudel, R.; Schmidt, H. *Chem. Ber*. **1994**, *127*, 1219.

(33) Steudel, R.; Hassenberg, K.; Münchow, V.; Schumann O.; Pickardt, J. *Eur. J. Inorg. Chem.* **2000**, 921.

(34) Wilson, E. B. *J. Chem. Phys*. **1939**, ***7***, 1047.

(35) Higgs, P. *Proc. R. Soc. London, Ser. A* **1953**, *220*, 472.

(36) Small, E. W.; Fanconi, B.; Peticolas, W. L. *J. Chem. Phys.* **1970**, *52*, 4369.

(37) Piseri, L.; Zerbi, G. *J. Chem. Phys.* **1968**, *48*, 3561.

(38) Tobin, M. C. *J. Chem. Phys.* **1955**, *23*, 891. Look also ref 29 in a quantum. mech. oligomer approach.

(39) Yildirim, V.; Ince, N. *J. Sound Vibration* **1997**, *204*, 311 and their refs 6, 8, 11, 18, 22, and 25.

(40) Schmidt, M. W.; Baldridge, K. K.; Boatz, J. A.; Elbert, S. T.; Gordon, M. S.; Jensen, J. H.; Koseki, S.; Matsunaga, N.; Nguyen, K. A.; Su, S.; Windus, T. L.; Dupuis, M.; Montgomery, J. A. *J. Comput. Chem.* **1993**, *14*, 1347.

(41) Ridge, D.; Becker, D.; Merkey, P. Sterling, T. *Beowulf: Harnessing the Power of Parallelism in a Pile of PCs*, Procceedings of the IEEE Aerospace Conference, 1997 (http://www.lobos.nih.gov).

(42) Granovsky, A. A. (www http://classic.chem.msu.su/gran/gamess/index.html).

(43) Frisch, M. J.; Trucks, G. W.; Schlegel, H. B.; Scuseria, G. E.; Robb, M. A.; Cheeseman, J. R.; Zakrzewski, V. G.; Montgomery, J. A., Jr.; Stratmann, R. E.; Burant, J. C.; Dapprich, S.; Millam, J. M.; Daniels, A. D.; Kudin, K. N.; Strain, M. C.; Farkas, O.; Tomasi, J.; Barone, V.; Cossi, M.; Cammi, R.; Mennucci, B.; Pomelli, C.; Adamo, C.; Clifford, S.; Ochterski, J.; Petersson, G. A.; Ayala, P. Y.; Cui, Q.; Morokuma, K.; Malick, D. K.; Rabuck, A. D.; Raghavachari, K.; Foresman, J. B.; Cioslowski, J.; Ortiz, J. V.; Stefanov, B. B.; Liu, G.; Liashenko, A.; Piskorz, P.; Komaromi, I.; Gomperts, R.; Martin, R. L.; Fox, D. J.; Keith, T.; Al-Laham, M. A.; Peng, C. Y.; Nanayakkara, A.; Gonzalez, C.; Challacombe, M.; Gill, P. M. W.; Johnson, B. G.; Chen, W.; Wong, M. W.; Andres, J. L.; Head-Gordon, M.; Replogle, E. S.; Pople, J. A. *Gaussian 98*, revision A.6; Gaussian, Inc.: Pittsburgh, PA, 1998.

(44) Dewar, M. J. S.; Thiel, W. *J. Am. Chem. Soc.* **1977**, *99*, 4899. Dewar, M. J. S.;. Reynolds, C. H *J. Comput. Chem*. **1986**, *7*, 140.

(45) Gordon, M. S.; Binkley, J. S.; Pople, J. A.; Pietro, W. J.; Hehre, W. J. *J. Am. Chem. Soc.* **1982**, *104*, 2797

(46) Hariharan, P. C.; Pople, J. A. *Theor. Chim. Acta* **1973**, *28*, 213. Francl, M. M.; Pietro, W. J.; Hehre, W. J. Binkley, J. S.; Gordon, M. S.; DeFrees, D. J.; Pople, J. A. *J. Chem. Phys.* **1982**, *77*, 3654.

(47) Lee, C.; Yang, W.; Parr, R. G. *Phys. Rev. B* **1988**, *37*, 785. Becke, A. D. *J. Chem. Phys.* **1993**, *98*, 5648

(48) Foresman, J. B.; Frisch, A. *Exploring Chemistry with Electronic Structure Methods*, 2nd ed.; Gaussian, Inc.: Pittsburgh, PA, 1996; p 64

(49) Schaftenaar, G.; Noordik, J. H. *Comput.-Aided Mol. Design* **2000**, *14*, 123.

(50) Hahn, J. *Z. Naturforsch. B* **1985**, *40*, 263.

(51) Steudel, R.; Strauss, R.; Jensen, D. *Chem.-Ztg*. **1985**, *109*, 349.

(52) Steudel, R.; Bergemann, K.; Buschmann, J.; Luger, P. *Angew. Chem., Int. Ed. Engl*. **1993**, *32*, 1702.

(53) Scmidt, H.; Steudel, R. *Z. Naturforsch*. **1990**, *45b*, 557.

(54) Ziegler, T. *Chem. Rev*. **1991**, *91*, 651.

(55) Andzelm, J.; Wimmer, E. *J. Chem Phys.* **1992**, *96*, 1280.

(56) Handy, N. C.; Murray, C. W.; Amos, R. D. *J. Phys. Chem.* **1993**, *97*, 4392.

(57) Johnson, B. G.; Gill, P. M. W.; Pople, J. A. *J. Chem Phys.* **1993**, *98*, 5612.

(58) Stephens, P. J.; Delvin, F. J.; Chabalowski, C. F.; Frisch, M. J. *J. Phys. Chem.* **1994**, *98*, 11623.

(59) Rauhut, G.; Pulay, P. *J. Phys. Chem.* **1995**, *99*, 3093.

(60) Finley, J. W.; Stephens, P. J. *J. Mol Struct. (THEOCHEM)* **1995**, *357*, 225.

(61) El Azhary, A. A.; Suter, H. U. *J. Phys. Chem.* **1996**, *100*, 15056.

(62) Wong, M. W. *Chem. Phys. Lett.* **1996**, *256*, 391.

(63) Liedtke, M.; Saleck, A. H.; Yamada, K. M. T.; Winnewisser, G.; Cremer, D.; Kraka, E.; Dolgner, A.; Hahn, J.; Dobos, S. *J. Phys. Chem.* **1993**, *97*, 11204.

(64) Raptis, S. G.; Nasiou, S. M.; Demetropoulos, I. N.; Papadopoulos, M. G. *J. Comput. Chem.* **1998**, *19*, 1698.

(65) Albinsson, B.; Antic. D.; Neumann, F.; Michl, J. *J. Phys. Chem. A* **1999**, *103*, 2184.

(66) Vos, M. H.; Rappaport, F.; Lambry, J. C.; Breton, J.; Martin, J. L. *Nature* **1993**, *363*, 320.

(67) Porto, M.; Urbakh, M.; Klafter, J. *Phys. Rev. Lett.* **2000**, *84*, 6058.

(68) Stratopoulos, G. N.; Dialynas T. E.; Tsironis G. P. *Phys. Lett. A* **1999**, *252*, 151.